^{18}F-FDG Uptake in Less Affected Lung Field Provides Prognostic Stratification in Patients with Interstitial Lung Disease

Tomomi Nobashi[1], Takeshi Kubo[1], Yuji Nakamoto[1], Tomohiro Handa[2], Sho Koyasu[1], Takayoshi Ishimori[1], Michiaki Mishima[2], and Kaori Togashi[1]

[1]Department of Diagnostic Imaging and Nuclear Medicine, Kyoto University Graduate School of Medicine, Kyoto, Japan; and
[2]Department of Respiratory Medicine, Kyoto University Graduate School of Medicine, Kyoto, Japan

This study evaluated the clinical significance of ^{18}F-FDG PET/CT in patients with interstitial lung disease (ILD), by investigating the relationships between ^{18}F-FDG PET/CT parameters and clinical indicators and by evaluating the prognostic implications of ^{18}F-FDG PET/CT results. **Methods:** Ninety patients (51 men, 39 women; mean age, 55.4 y; age range, 26–78 y) with ILD who underwent ^{18}F-FDG PET/CT were retrospectively analyzed. SUV_{mean} was defined as the mean SUV of the less-affected lung field, SUV_{TF} as adjusted SUV_{mean} using tissue fraction (TF), and CT_{mean} as the mean attenuation of the corresponding region of interest on high-resolution CT. SUV_{mean}, SUV_{TF}, and CT_{mean} were compared in the 90 ILD patients and in 15 age- and sex-matched controls. Correlations of SUV_{max}, SUV_{mean}, SUV_{TF}, and CT_{mean} with clinical indicators, including estimated percentage of forced vital capacity (%FVC), estimated percentage of diffusion capacity of the lungs for carbon monoxide (%DLco), sialylated carbohydrate antigen Krebs von den Lungen-6 (KL-6), surfactant protein D (SP-D), C-reactive protein (CRP), lactate dehydrogenase (LDH), and ILD-sex-age-physiology (GAP) index, were evaluated using the Spearman rank correlation test and the Tukey–Kramer test. A Cox proportional hazards model was used for univariate and multivariate analyses of factors associated with lung transplantation-free survival. **Results:** SUV_{mean}, SUV_{TF}, and CT_{mean} were significantly higher in ILD patients than in healthy controls, except for CT_{mean} in patients with a nonusual interstitial pneumonia pattern. SUV_{mean} and CT_{mean} were significantly correlated with %FVC, %DLco, KL-6, and SP-D; SUV_{TF} was significantly correlated with %DLco, KL-6, SP-D, and LDH; and SUV_{max} was weakly correlated with KL-6 and CRP. Univariate analysis showed that SUV_{mean}, SUV_{TF}, sex, %FVC, %DLco, KL-6, and ILD-GAP index were significantly prognostic of lung transplantation-free survival; and multivariate analysis showed that SUV_{mean} and ILD-GAP index were independently prognostic of lung transplantation-free survival. A higher SUV_{mean} indicated a poorer prognosis, especially in patients with moderate risk based on ILD-GAP index. **Conclusion:** SUV_{mean} was significantly but moderately correlated with clinical indicators, providing independent prognostic information in patients with ILD. ^{18}F-FDG PET/CT may be helpful for monitoring and risk stratification of ILD patients.

Interstitial lung disease (ILD) is a chronic progressive pulmonary disease of unknown etiology. Because no effective therapy has yet been developed, careful evaluation and management are critically important in maintaining quality of life and in reducing mortality. Irrespective of ILD type, disease severity is generally evaluated by pulmonary function tests (PFTs); disease extension by chest high-resolution CT (HRCT); and inflammation and disease progression by laboratory tests, such as measures of C-reactive protein (CRP), lactate dehydrogenase (LDH), sialylated carbohydrate antigen Krebs von den Lungen-6 (KL-6), and surfactant protein D (SP-D). Recently, a simple sex-age-physiology (GAP) risk-prediction model was developed for idiopathic pulmonary fibrosis (IPF) (1), and a modified ILD-GAP model was developed for chronic ILD (2). These models have been proved feasible, enabling comprehensive risk assessment of patients with ILD (3–5).

At present, HRCT is an essential clinical imaging modality for evaluating ILD, distinguishing IPF from other types of ILD and determining precise architectural changes. Moreover, quantitative analysis of HRCT results was found to correlate with lung function, exercise testing, KL-6 concentration, and patient quality of life (6,7).

To date, the significance of ^{18}F-FDG uptake in ILD has not been fully investigated. Because ^{18}F-FDG accumulates in benign hypermetabolic foci, including inflammatory foci, as well as in neoplasms, ^{18}F-FDG is used to evaluate patients with various benign diseases (8,9).

ILD is characterized by areas of both interstitial inflammation and fibrotic changes (10,11), suggesting that ^{18}F-FDG accumulation may be associated with disease activity in patients with ILD (12–15). In addition, increased ^{18}F-FDG uptake in areas of apparently normal pulmonary parenchyma on HRCT was observed in patients with IPF (16). This finding suggested that higher ^{18}F-FDG uptake by less-affected lung tissue may provide additional clinical information in patients with ILD, in addition to the morphologic changes observed by HRCT. This study hypothesized that ^{18}F-FDG accumulation in lung areas close to normal-appearing on CT may represent disease activity and may be used for risk stratification and management of patients with ILD. To assess the clinical
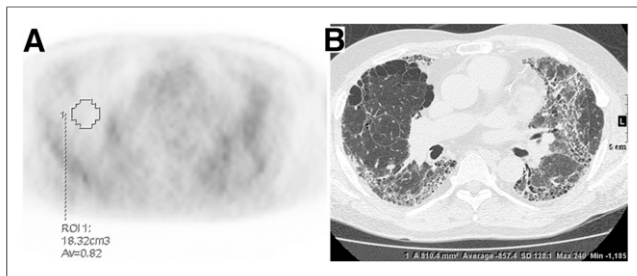
FIGURE 1. Representative images of VOIs and region of interest for SUV_{mean} and CT_{mean}. (A) VOI of 18 cm^3 was manually placed on background lung field of PET image, and SUV_{mean} was automatically calculated as 0.82 on a workstation. (B) Corresponding region of interest was manually placed on HRCT image, and CT_{mean} was automatically calculated as −857.

efficacy of ^{18}F-FDG PET/CT in patients with ILD, this study investigated the relationships between ^{18}F-FDG PET/CT imaging parameters and clinical indicators in patients with ILD as well as evaluated the prognostic implications of ^{18}F-FDG PET/CT results.

MATERIALS AND METHODS

Patients

This retrospective study included 275 patients with known or suspected ILD who underwent ^{18}F-FDG PET/CT to exclude malignancy between May 2009 and June 2015. Patients were included if they were pathologically or clinically diagnosed with ILD. Patients were excluded if they had any malignancy or inflammation, except for PET-diagnosed ILD; they had a history of other malignancies; or they had blood glucose levels greater than 200 mg/dL just before ^{18}F-FDG injection. Of these 275 patients, 185 were excluded, including 147 with an existing malignancy or history of malignancy, 20 with infectious changes, 15 with high blood sugar levels, and 3 not diagnosed with ILD. The study therefore included 90 patients, consisting of 51 men and 39 women, with a mean age of 55.4 y (age range, 26–78 y).

To evaluate ^{18}F-FDG tissue uptake and lung density of apparently normal or less-affected area in ILD patients, normal age- and sex-matched control patients were selected from the records of the same PET facility. These 15 controls, comprising 8 men and 7 women, with a mean age of 56 y (age range, 29–66 y), all had extrathoracic lymphoma but were in remission. Medical records showed that none had any known respiratory disease, with all undergoing both PET and conventional chest CT within 6 mo.

This retrospective study was approved by the institutional review board of Kyoto University Graduate School of Medicine. Written informed consent was obtained from each patient regarding access to his or her data.

PET Image Acquisition

PET scanning was performed using a combined PET/CT scanner (Discovery ST Elite; GE Healthcare). All patients fasted for 4 h or more before the administration of ^{18}F-FDG. Whole-body PET scanning, from the level of the thigh to that of the head, was started approximately 60 min after injection of a dose of 3.7 MBq/kg of ^{18}F-FDG. CT scans of the same areas were acquired, using approximately 30 mAs of current time product. Both PET and CT scans were obtained under conditions of shallow breathing. PET images were reconstructed with CT-derived attenuation correction using an iterative reconstruction algorithm (2 iterations, 12 subsets).

CT Image Acquisition

Eighty-three patients underwent noncontrast chest HRCT within 6 mo before or after ^{18}F-FDG PET/CT. These HRCT findings were also

included in the analysis to compare the associations of PET and CT parameters with ILD. Images were acquired with a 1-mm slice thickness, a 0.5-s rotation time, a beam pitch of 0.83, and 120 kVp of x-ray tube voltage. The tube current was determined by automatic exposure control, which is clinically used for dose reduction.

Image Analysis

PET images were displayed on a workstation (Advantage Workstation, version 4.6; GE Healthcare). Observers were masked to clinical information, except for the diagnosis of ILD. SUV was calculated as (decay-corrected activity/tissue volume)/(injected dose/body weight). Three PET parameters were calculated: SUV_{max}, SUV_{mean}, and $SUV_{tissue\ fraction\ (TF)}$. SUV_{max} was defined as the highest SUV in each hypermetabolic ILD lesion. SUV_{mean} was measured in 1 target volume of interest (VOI), which was placed at the most normal-appearing area in the lungs of each subject. The target VOIs had a fixed spherical shape measuring 18 cm^3 (16). The area occupied by the VOI typically shows no or minimal signs of increased attenuation on CT (Fig. 1). If normal lung parenchyma was not observed, the area showing the faintest ground-glass opacity was selected for the VOI. VOIs were carefully placed so that no voxel in the VOI was located in the mediastinum, chest wall, or area of lung parenchyma with emphysematous changes or trapped air. Because increased ^{18}F-FDG accumulation is often observed at posterior areas of the lung accompanied by dependent lung opacity, VOIs also carefully avoid areas affected by gravity. Hence, SUV_{mean} represents the uptake by apparently normal or less-affected lung parenchyma in each patient. SUV_{TF} has been introduced as a TF-corrected SUV in a recent article, to demonstrate

TABLE 1
Patient Demographic and Clinical Characteristics

Characteristic	
Mean age ± SD (y)	55.4 ± 11.0
Sex (male:female)	51:39 (56.7%:43.3%)
Lung transplantation (Yes:No)	18:72 (20.0%:80.0%)
Type of ILD	
IPF	24 (26.7%)
Unclassifiable ILD	7 (7.8%)
CT-ILD/idiopathic NSIP	55 (61.1%)
Chronic HP	4 (4.4%)
PFT	
Mean %FVC ± SD (n = 75; %)*	58.1 ± 22.1
Mean %DLco ± SD (n = 61; %)*	29.9 ± 15.7
ILD-GAP index (n = 75)*	
0	9 (12.0%)
1	15 (20.0%)
2	25 (33.3%)
3	19 (25.3%)
4	7 (9.3%)
5–8	0
Median observation period (d)	395 (range, 2–2,392)

*Because data were not acquired during designated period, numbers do not total 90.

NSIP = nonspecific interstitial pneumonia; HP = hypersensitivity pneumonitis.

TABLE 2
PET and CT Imaging Parameters in Included Patients

Image parameters	Values
Mean $SUV_{max} \pm SD$ ($n = 90$)	2.46 ± 0.76
Mean $SUV_{mean} \pm SD$ ($n = 90$)	0.60 ± 0.24
Mean $SUV_{TF} \pm SD$ ($n = 90$)	2.44 ± 0.50
Mean $CT_{mean} \pm SD$ (HU) ($n = 83$)	-833 ± 68

TF = tissue fraction.

more appropriate metabolic characteristics independent of degree of aeration (*17*). SUV_{TF} was calculated using the parameter k, a coefficient representing the proportion of stromal component in the targeted VOI, applying the CT image acquired on the PET/CT scan. In this study, SUV_{TF} was defined as below using the mean Hounsfield units (HU) of corresponding lung area.

$$k = \frac{HUlung - HUair}{HUtissue - HUair}, SUV_{TF} = \frac{SUVmean}{k}$$

CT_{mean} was calculated as the mean CT attenuation, in HUs, of the region of interest corresponding to the maximum cross section of the VOI of SUV_{mean}. SUV_{mean}, SUV_{TF}, and CT_{mean} were assessed by 2 board-certified radiologists with 7 and 20 y of experience, respectively, to determine interobserver agreement.

Clinical Data

Patients underwent PFTs, including estimated percentage of forced vital capacity (%FVC) and estimated percentage of diffusion capacity of the lungs for carbon monoxide (%DLco), within 6 mo of PET. The ILD-GAP index was also evaluated. This index has been proposed as a single clinical prediction model that accurately estimates mortality across multiple chronic ILD subtypes. The ILD-GAP index includes predictors, such as ILD subtype, sex, age, physiology, and PFT results, and is scored as described (*2*), with IPF, unclassified ILD, male sex, age greater than 65 y, and reduced %FVC and %DLco having high scores. Scores on the ILD-GAP index range from 0 to 8. ILD was characterized into 2 patterns, a usual interstitial pneumonia (UIP) pattern, corresponding to IPF and unclassifiable ILD, and a non-UIP pattern, corresponding to connective tissue disease associated with interstitial lung disease (CT-ILD)/idiopathic nonspecific interstitial pneumonia and chronic hypersensitivity pneumonitis.

Available clinical laboratory data, including concentrations of CRP, LDH, KL-6, and SP-D, were obtained from patients' medical records. To evaluate the correlations of these parameters with ^{18}F-FDG uptake, only those data obtained within 14 d of PET and without any change in medication were analyzed. The correlations between CT_{mean} and laboratory data obtained within 14 d of chest HRCT were also evaluated. Transplantation-free survival (TFS) was calculated from PET and HRCT scan dates to date of death, transplantation, or last follow-up.

Statistical Analysis

The normality of SUV_{mean}, SUV_{TF}, and CT_{mean}, as determined by the 2 evaluators, was assessed with the Kolmogorov–Smirnov test. Correlations between interpreters were evaluated with the Pearson correlation test. To confirm differences in apparently normal or less-affected tissue of ILD patients and healthy controls, SUV_{mean} and CT_{mean} in ILD patients with the UIP and non-UIP patterns and in control subjects were compared using the Dunn test. The relationships between imaging parameters (SUV_{max}, SUV_{mean}, SUV_{TF}, and CT_{mean}) and clinical parameters (%FVC, %DLco, KL-6, SP-D, LDH, and CRP) were evaluated by the Spearman rank correlation test. The relationships of these 4 imaging parameters with the ILD-GAP index were evaluated by the Tukey–Kramer method. To distinguish patients with favorable and poorer prognoses, optimal cutoffs of SUV_{max}, SUV_{mean}, SUV_{TF}, and CT_{mean} for TFS were determined by receiver-operating-characteristic (ROC) analysis, and these cutoffs were used in generating Kaplan–Meier curves. The associations of TFS with these imaging and clinical parameters were assessed using univariate and multivariate Cox proportional hazards models. To avoid overfitting the model, the number of variables for multivariate analysis was determined as described (*5*). That is, no more than 1 independent variable for every 10 uncensored outcomes in the derivation cohort was considered for inclusion in the final multivariate model. Therefore, the clinical indices with the lowest *P* values in univariate analysis and that satisfied the above-mentioned criteria were selected for multivariate analysis. Finally, to confirm the prognostic power of imaging parameters significant in multivariate analysis, Kaplan–Meier curves were generated for groups of patients with low and moderate scores on the ILD-GAP index using the optimal cutoff value calculated by ROC analysis, and survival differences were assessed using the log-rank test. Two-sided *P* values of less than 0.05 were considered statistically significant. All statistical analyses were performed using JMP pro 11 software (SAS Institute Inc.).

RESULTS

Patients

The characteristics of the included patients are shown in Tables 1 and 2 and in Supplemental Tables 1 and 2 (supplemental materials
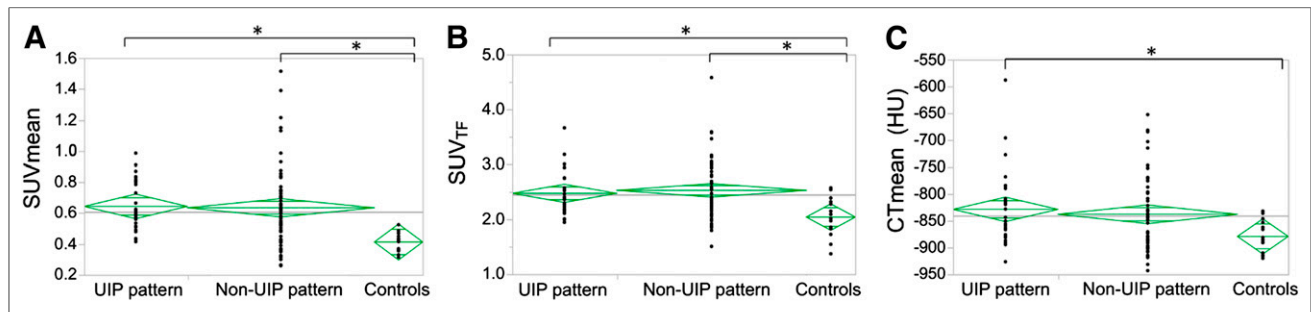
FIGURE 2. SUV_{mean} (A), SUV_{TF} (B), and CT_{mean} (C) of ILD patients with UIP pattern, non-UIP pattern, and healthy controls. Horizontal bars in each rhombus represent 25th, 50th, and 75th percentiles from top. *$P < 0.016$ (Bonferroni adjustment).

TABLE 3
Correlations Between Imaging Parameters and Clinical Factors

Image parameters	%FVC	%DLco	KL-6	SP-D	CRP	LDH
SUV_{max}	NS	NS	0.29 (0.014)	NS	0.22 (0.043)	NS
SUV_{mean}	−0.45 (<.0001)	−0.46 (0.0002)	0.56 (<.0001)	0.36 (0.0098)	NS	NS
SUV_{TF}	NS	−0.29 (0.022)	0.41 (0.0003)	0.29 (0.040)	NS	0.066 (0.040)
CT_{mean}	−0.50 (<.0001)	−0.40 (0.0028)	0.29 (0.019)	0.40 (0.0060)	NS	NS

NS = not significant; TF = tissue fraction.
Rho (ρ) values are demonstrated. *P* values are in parentheses.

are available at http://jnm.snmjournals.org). All mean progression-free survival and laboratory results were higher than their reference range. The median follow-up period was 395 d (range, 2–2,392 d). No patient showed acute exacerbation on the day of PET or CT. The Dunn test showed that SUV_{max}, SUV_{mean}, and SUV_{TF} did not differ significantly in groups of patients receiving different therapy regimens (Supplemental Table 3).

Interobserver Agreement

All of the imaging parameters in less-affected lung fields were normally distributed (SUV_{mean}, *P* = 0.87; SUV_{TF}, *P* = 0.12; and CT_{mean}, *P* = 1.00), with a significant and strong positive correlation between the 2 observers (SUV_{mean}, R^2 = 0.91, *P* < 0.0001; SUV_{TF}, R^2 = 0.74, *P* < 0.0001; and CT_{mean}, R^2 = 0.83, *P* < 0.0001). The averages of these parameters assessed by the 2 observers were used in subsequent analyses.

Comparisons of SUV_{mean}, SUV_{TF}, and CT_{mean} in ILD Patients and Healthy Controls

SUV_{mean} and SUV_{TF} were significantly higher in patients with the UIP (*P* = 0.0008 and *P* = 0.0074, respectively) and non-UIP (*P* < 0.0001 and *P* = 0.0014, respectively) patterns than in healthy controls. In contrast, CT_{mean} was significantly higher in patients with the UIP (*P* = 0.018) but not with the non-UIP pattern than in controls. SUV_{mean}, SUV_{TF}, and CT_{mean} did not differ significantly in patients with the UIP and non-UIP patterns (Fig. 2).

Correlations of SUV_{max}, SUV_{mean}, SUV_{TF}, and CT_{mean} with Clinical Parameters

Table 3 and Supplemental Figure 1 show the correlations between imaging parameters and clinical indices. SUV_{mean} showed

moderate negative correlations with %FVC and %DLco, a moderate positive correlation with KL-6, and a weak correlation with SP-D, but no correlations with CRP and LDH. SUV_{TF} showed a moderate correlation with KL-6 and weak correlations with %DLco, SP-D, and LDH. CT_{mean} showed moderate correlations with %FVC, %DLco, and SP-D and a weak correlation with KL-6. SUV_{max} showed significant but weak correlations with KL-6 and CRP. SUV_{mean} was significantly higher in the group with an ILD-GAP index of 4 than in the groups with ILD-GAP indices of 0 (*P* = 0.018) and 1 (*P* = 0.022).

Prognostic Implications

When optimal cutoff values derived from ROC analyses were used, SUV_{mean} (cutoff, 0.62; area under the curve [AUC], 0.714), SUV_{TF} (cutoff, 2.57; AUC, 0.709), and ILD-GAP index (cutoff, 2; AUC, 0.721) were significantly associated with TFS, whereas SUV_{max} and CT_{mean} were not. Kaplan–Meyer analyses using these cutoffs for SUV_{mean}, SUV_{TF}, and ILD-GAP index showed significant differences in TFS (Fig. 3). Univariate analysis showed that SUV_{mean}, SUV_{TF}, sex, %FVC, %DLco, KL-6, and ILD-GAP index were significant prognostic factors of TFS (Table 4). Univariate analysis showed that %DLco and ILD-GAP index were candidate predictors of TFS; however, only 17 and 21 patients were uncensored for %DLco and ILD-GAP index, respectively. Therefore, multivariate analysis was performed using ILD-GAP index, not with %DLco. This analysis showed that SUV_{mean} and ILD-GAP index were independently prognostic of TFS (Table 5). Because SUV_{mean} was significantly correlated with clinical parameters, such as %FVC, KL-6, and SP-D, a multivariate analysis that included SUV_{mean} and these clinical parameters was performed,
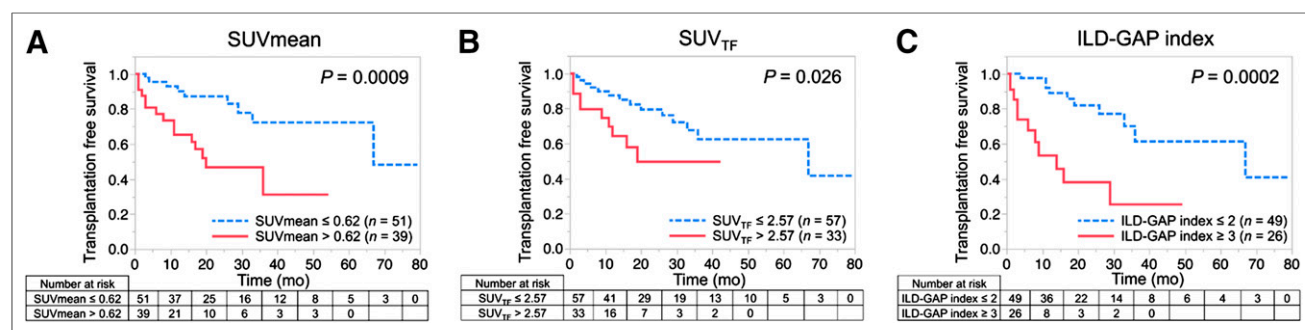
FIGURE 3. Kaplan–Meier analysis of SUV_{mean} (≤0.62 vs. >0.62) (A), SUV_{TF} (≤2.57 vs. >2.57) (B), and ILD-GAP index (<3 vs. ≥3) (C) as predictors of TFS in patients with ILD. Patients with higher SUV_{mean} (>0.62), higher SUV_{TF} (>2.57), and higher ILD-GAP index (≥3) had significantly poorer prognosis.

TABLE 4
Univariate Analysis of Factors Associated with TFS

Variable	n	HR	95% CI	P
Age	90	1.00	0.96–1.03	0.81
Sex	90	3.47	1.44–9.65	0.0047*
UIP or non-UIP pattern	90	0.70	0.25–1.71	0.45
%FVC	75	0.97	0.95–0.99	0.0087*
%DLco	61	0.93	0.88–0.97	0.0002*
ILD-GAP index	75	2.28	1.44–3.82	0.0003*
KL-6	73	1.00	1.00–1.00	0.049*
SP-D	49	1.00	1.00–1.01	0.050
CRP	85	0.81	0.52–1.05	0.13
LDH	83	1.00	1.00–1.00	0.87
SUV_{max}	90	0.97	0.58–1.62	0.91
SUV_{mean}	90	51.0	8.24–306	<0.0001*
SUV_{TF}	90	3.08	1.42–6.26	0.0055*
CT_{mean}	84	1.00	1.00–1.01	0.059

*$P < 0.05$.
HR = hazard ratio; CI = confidence interval; TF = tissue fraction.

showing that SUV_{mean} was an independent prognostic factor for TFS. To assess the prognostic value of SUV_{mean} when coupled with ILD-GAP index, patients were divided into 2 groups, those with ILD-GAP indices of 0–2 and those with ILD-GAP indices of 3–4. SUV_{mean} cutoff values were determined by ROC analysis for each ILD-GAP index subgroup, and Kaplan–Meier curves were generated on the basis of these SUV_{mean} cutoffs (Fig. 4). SUV_{mean} was not prognostic in patients with an ILD-GAP index of 0–2. However, in the moderate-risk group, consisting of patients with an ILD-GAP index of 3–4, patients with higher SUV_{mean} had significantly poorer prognosis than those with lower SUV_{mean}.

DISCUSSION

The present study investigated the clinical importance of PET and CT parameters calculated from apparently normal or less-affected lung tissue in patients with interstitial pneumonia. Both ^{18}F-FDG accumulation and CT attenuation in less-affected lung fields were significantly higher in patients with ILD than in healthy controls but did not differ significantly in ILD patients with UIP and non-UIP patterns. Among the imaging parameters, SUV_{mean} showed significant correlations with clinical factors and prognosis. To our knowledge, this is the first study to show that a PET parameter had an add-on effect to ILD-GAP index in the risk stratification of patients with ILD.

This study found that SUV_{mean} was significantly correlated with various clinical factors, including %FVC, %DLco, KL-6, and SP-D. SUV_{mean} was previously shown to be related to the activity or severity of ILDs (13–15). Moreover, SUV_{mean} significantly affected prognosis, not only being an independent prognostic factor but also stratifying mortality in patients with moderate scores on the ILD-GAP index. The ILD-GAP index is regarded as a strong risk-stratification model in patients with ILDs, with this study finding that SUV_{mean} had add-on value in risk stratification in patients with an ILD-GAP index of 3–4 but not in those with an

ILD-GAP index of 0–2. The latter finding may have been due to the short follow-up period, with 39 of 49 patients censored in the Kaplan–Meyer analysis. Full evaluation of the prognostic power of SUV_{mean} requires longer follow-up time for low-risk patients.

Previous studies have shown the value of CT image analyses in patients with ILD. For example, a quantitative stratification paradigm based on characteristic radiologic patterns was found to identify subsets of diffuse pulmonary lung disease patients (4). Relative CT values ranging from −700 to −301 HUs were found to closely correlate with KL-6 concentrations in patients with polymyositis and dermatomyositis (6), and lung CT densitometry and PFT were found to correlate in patients with systemic sclerosis (7). These results indicate that CT densitometry provides important predictive information in patients with ILD.

The mechanisms underlying the correlations between ^{18}F-FDG accumulation and less-affected lung tissue have not been determined; however, ^{18}F-FDG uptake likely provides an additional value not obtained by HRCT. The process of fibrosis formation commonly seen in ILDs begins with the migration of activated fibroblasts and inflammatory cells from the alveolar interstitium, followed by connective tissue synthesis on the luminal side of the epithelial basement membrane (18). This mechanism would lead to ^{18}F-FDG avidity, because ^{18}F-FDG accumulation is increased in active inflammatory lesions, which include young fibroblasts, endothelial cells of vessels, and macrophages (19). ^{18}F-FDG PET would therefore reveal worsening of disease, before the detection of morphologic changes on HRCT.

We found, however, that CT_{mean} and SUV_{TF} did not show the strong relationships to clinical indicators shown by SUV_{mean}. CT_{mean} was moderately correlated with PFT and SP-D and weakly correlated with KL-6 but was not significantly correlated with patient prognosis. SUV_{TF}, which reflects ^{18}F-FDG accumulation in lung tissue without the influence of CT attenuation (17), showed significant correlations with %DLco, KL-6, and SP-D, but these correlations were weaker than those shown by SUV_{mean}. Although univariate analysis showed that SUV_{TF} was a prognostic factor, multivariate analysis showed that it was not an independent predictor. These findings suggest that information obtained from either CT attenuation or ^{18}F-FDG accumulation alone in lung tissue is somewhat related to ILDs but has limited utility in disease evaluation. In contrast, SUV_{mean} would be practically useful for disease evaluation.

SUV_{max} showed only weak correlations with KL-6 and CRP and did not significantly correlate with LDH. CRP and LDH are common markers of active inflammation and were expected to correlate with SUV_{max}, which indicates an active inflammatory

TABLE 5
Multivariate Analysis of Factors Associated with TFS

Model	n	Variable	P
SUV_{mean} and ILD-GAP index	75	SUV_{mean}	0.0068*
		ILD-GAP index	0.0017*
SUV_{TF} and ILD-GAP index	75	SUV_{TF}	0.44
		ILD-GAP index	0.0006*

*$P < 0.05$.
TF = tissue fraction.
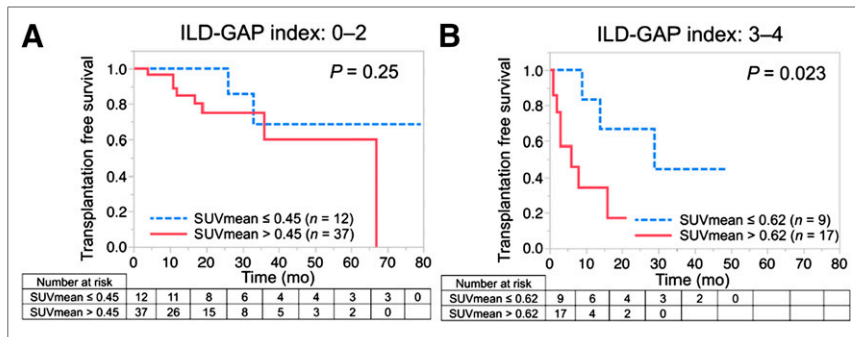
FIGURE 4. Kaplan–Meier analysis of SUV$_{mean}$ as predictor of TFS in groups of patients with ILD-GAP index of 0–2 (A) and 3–4 (B). In patients with ILD-GAP index of 0–2, there was no difference in TFS between patients with higher (>0.45) and lower (≤0.45) SUV$_{mean}$. In group with moderate mortality risk (ILD-GAP index 3–4), however, patients with higher SUV$_{mean}$ (>0.62) had significantly poorer TFS than those with lower SUV$_{mean}$ (≤0.62).

site. This poor correlation may have been due, at least in part, to the inclusion in this study of patients with CT-ILD, who may have had an active inflammatory site outside the lungs not detectable by PET/CT. Moreover, measurements of SUV$_{max}$ in areas with dependent lung opacity would have resulted in the inclusion areas of apparently increased accumulation without inflammation. Therefore, our results do not necessarily indicate that SUV$_{max}$ is poorly correlated with clinical factors or prognosis. Further studies are needed to determine the usefulness of SUV$_{max}$.

This study had several limitations. First, because of the retrospective study design, the therapy regimen was not uniform and the effect of therapy was not considered. Second, patients with high-risk scores (ILD-GAP index ≥ 5) were not included; therefore, the significance of PET parameters in patients with higher ILD-GAP scores is yet to be clarified. To our knowledge, however, this study included the largest number of patients with ILD evaluated by ^{18}F-FDG PET. Third, patients with IPF and other types of ILD were pooled because of the small number of patients with each indication. Inflammatory changes are not as prominent in IPF as in other ILDs, such as CT-ILD and chronic hypersensitivity pneumonitis. Fourth, the selected VOI may not have accurately reflected the exact activity of ILD, although there was interobserver validation of the setting of VOI to enhance reproducibility.

Considered overall, SUV$_{mean}$ calculated in less-affected lung fields was strongly related to clinical indicators and prognosis in patients with ILD. SUV$_{mean}$ provides information on both CT attenuation and ^{18}F-FDG accumulation, suggesting it may be practically useful for the management of ILD. This study, however, did not investigate the mechanism underlying how SUV$_{mean}$ affects the prognosis of ILD. Furthermore, the relationships of SUV$_{mean}$ with acute exacerbation and prediction of disease progression require clarification. Additional prospective studies, including larger numbers of patients, are required.

CONCLUSION

Both ^{18}F-FDG accumulation and CT attenuation in apparently normal or less-affected lung tissue were higher in patients with ILD than in healthy controls. SUV$_{mean}$ was moderately but significantly correlated with clinical indicators and was independently prognostic of lung TFS. PET analysis of ^{18}F-FDG accumulation on PET may contribute to risk stratification of ILD, especially in patients with moderate mortality risk.

REFERENCES

1. Ley B, Ryerson CJ, Vittinghoff E, et al. A multidimensional index and staging system for idiopathic pulmonary fibrosis. *Ann Intern Med.* 2012;156:684–691.
2. Ryerson CJ, Vittinghoff E, Ley B, et al. Predicting survival across chronic interstitial lung disease: the ILD-GAP model. *Chest.* 2014;145:723–728.
3. Kim ES, Choi SM, Lee J, et al. Validation of the GAP score in Korean patients with idiopathic pulmonary fibrosis. *Chest.* 2015;147:430–437.
4. Raghunath S, Rajagopalan S, Karwoski RA, et al. Quantitative stratification of diffuse parenchymal lung diseases. *PLoS One.* 2014;9:e93229.
5. Ley B, Elicker BM, Hartman TE, et al. Idiopathic pulmonary fibrosis: CT and risk of death. *Radiology.* 2014;273:570–579.
6. Ozuno NT, Akamatsu H, Takahashi H, Fujii N, Yoshida S. Quantitative diagnosis of connective tissue disease-associated interstitial pneumonia using thoracic computed tomography images. *Clin Rheumatol.* 2015;34:2113–2118.
7. Camiciottoli G, Orlandi I, Bartolucci M, et al. Lung CT densitometry in systemic sclerosis: correlation with lung function, exercise testing, and quality of life. *Chest.* 2007;131:672–681.
8. Courtois A, Nusgens BV, Hustinx R, et al. ^{18}F-FDG uptake assessed by PET/CT in abdominal aortic aneurysms is associated with cellular and molecular alterations prefacing wall deterioration and rupture. *J Nucl Med.* 2013;54:1740–1747.
9. Nakatsuka Y, Handa T, Nakamoto Y, et al. Total lesion glycolysis as an IgG4-related disease activity marker. *Mod Rheumatol.* 2015;25:579–584.
10. Wolters PJ, Collard HR, Jones KD. Pathogenesis of idiopathic pulmonary fibrosis. *Annu Rev Pathol.* 2014;9:157–179.
11. Travis WD, Costabel U, Hansell DM, et al. An official American Thoracic Society/European Respiratory Society statement: update of the international multidisciplinary classification of the idiopathic interstitial pneumonias. *Am J Respir Crit Care Med.* 2013;188:733–748.
12. Nusair S, Rubinstein R, Freedman NM, et al. Positron emission tomography in interstitial lung disease. *Respirology.* 2007;12:843–847.
13. Groves AM, Win T, Screaton NJ, et al. Idiopathic pulmonary fibrosis and diffuse parenchymal lung disease: implications from initial experience with ^{18}F-FDG PET/CT. *J Nucl Med.* 2009;50:538–545.
14. Lee EY, Wong CS, Fung SL, Yan PK, Ho JC. SUV as an adjunct in evaluating disease activity in idiopathic pulmonary fibrosis: a pilot study. *Nucl Med Commun.* 2014;35:631–637.
15. Uehara T, Takeno M, Hama M, et al. Deep-inspiration breath-hold ^{18}F-FDG-PET/CT is useful for assessment of connective tissue disease associated interstitial pneumonia. *Mod Rheumatol.* 2016;26:121–127.
16. Win T, Thomas BA, Lambrou T, et al. Areas of normal pulmonary parenchyma on HRCT exhibit increased FDG PET signal in IPF patients. *Eur J Nucl Med Mol Imaging.* 2014;41:337–342.
17. Lambrou T, Groves AM, Erlandsson K, et al. The importance of correction for tissue fraction effects in lung PET: preliminary findings. *Eur J Nucl Med Mol Imaging.* 2011;38:2238–2246.
18. Fukuda Y, Ferrans VJ, Schoenberger CI, Rennard SI, Crystal RG. Patterns of pulmonary structural remodeling after experimental paraquat toxicity: the morphogenesis of intraalveolar fibrosis. *Am J Pathol.* 1985;118:452–475.
19. Yamada S, Kubota K, Kubota R, Ido T, Tamahashi N. High accumulation of fluorine-18-fluorodeoxyglucose in turpentine-induced inflammatory tissue. *J Nucl Med.* 1995;36:1301–1306.